



# OPEN Investigation of the preparation of iron sulfate-loaded niosomes by an experimental novel method

Samira Khalil Abadi<sup>1</sup>, Kiana Peyvandi<sup>1✉</sup> & Sheida Shariat<sup>2</sup>

Iron is a crucial nutrient for our bodies, and its absence can lead to serious health issues like anemia. Unfortunately, oral iron supplements are frequently poorly absorbed and can lead to gastrointestinal discomfort due to iron's oxidative properties. However, using nanocarrier systems to encapsulate iron can mitigate these issues, enhancing its absorption and protecting it from oxidation, ultimately improving its effectiveness. In this research, niosomes loaded with iron sulfate were prepared using surfactant span 60 and Tween 80 via thin film hydration method. Cholesterol and 1-Dodecanol were used as stabilizers in different ratios. Physiochemical properties of niosomes loaded with iron sulfate, such as particle size, polydispersity index (PDI), zeta potential, and encapsulation efficiency (EE%), were investigated. The vesicle sizes varied between 453 and 3,276 nm, with encapsulation efficiencies ranging from 75 to 93%. The zeta potential measured between  $-9.91$  and  $6.3$  mV, while the particle size distribution (PDI) was observed to be between 0.004 and 0.59 in a phosphate buffer solution at pH 6.8. Ultimately, F1 Formula was established as the most effective formula, achieving an efficiency of 90.8%, a particle size of 546.8 nm, a zeta potential of 5.5, and a PDI of 0.57.

**Keywords** Drug delivery, Iron encapsulation, Niosome, Iron deficiency anemia, Ferrous sulfate

Iron is an essential nutrient in the human diet and a vital part of metalloproteins (hemoglobin, myoglobin, ferritin, transferrin, cytochromes, etc.), which exists for the transport of  $O_2$  to tissues, transport of  $CO_2$ , as well as formation of red blood cells, redox reactions, electron transport, cellular energy production, gene regulation. It is also as an essential synthetic group for regulating, activating, and controlling many enzymatic reactions (enzymes such as cytochrome oxidase, catalase)<sup>1–5</sup>. Inadequate intake of iron from the diet or poor absorption of iron from the gastrointestinal tract from food causes iron deficiency, which is the most common nutritional problem in the world and can lead to some disorders such as anemia, immune system disorders, or pregnancy complications. Children, teenagers, and especially women of childbearing age are at risk of suffering from iron deficiency anemia, and the only solution is to increase iron consumption either through supplementation or fortification<sup>6–10</sup>.

Currently, oral iron supplements, such as ferrous sulfate, ferrous gluconate, and ferrous fumarate, are usually used to treat diseases related to iron deficiency. However, oral iron supplements are often ineffectively absorbed and potentially cause adverse effects in the gastrointestinal tract primarily due to the oxidative toxicity of iron<sup>11–14</sup>.

Encapsulating or trapping iron in vesicles and other nanocarrier systems not only reduces organoleptic problems but also protects iron from oxidation caused by external factors, while also reducing its interaction with other components. It prevents the direct contact of iron with the digestive system, thus improving its bioavailability and intestinal absorption. In addition to mitigating side effects, encapsulation provides targeted delivery and slow release; thus, lower doses of iron cause a therapeutic effect<sup>15–18</sup>.

Niosomes are a new type of nanocarrier systems that are formed by the self-assembly of non-ionic surfactants in aqueous environments, which leads to closed bilayer structures. These nanovesicles can trap hydrophilic, hydrophobic, and amphiphilic compounds resulted in many applications in the food, pharmaceutical, and cosmetic industries<sup>19–22</sup>. Hydrophilic compounds are trapped in aqueous compartments between two layers, while lipophilic compounds are preferably placed in two surfactant layers<sup>23–25</sup>. Compared to phospholipid compounds that are usually used in liposomes, niosomes have attracted the attention of researchers thanks to their lower cost and higher stability during storage, flexibility in structure, etc. It has become a suitable carrier for loading many drugs, nutrients, genes, protein and peptide compounds, etc<sup>26,27</sup>.

<sup>1</sup>Faculty of Chemical, Petroleum and Gas Engineering, Semnan University, Semnan, Iran. <sup>2</sup>Department of Pharmacy, Damghan Branch, Islamic Azad University, Damghan, Iran. ✉email: k\_peyvandy@semnan.ac.ir

In their research, Gutiérrez et al. have introduced several formulations for trapping iron in niosomes. They made iron-sulfate containing niosomes through a modified ethanol injection method and three surfactants, Peceol, Plurol Oleique, and Span 80<sup>8</sup>. Indeed, our aim of this study is to expand Gutiérrez et al.'s research to produce niosomes containing iron sulfate, via thin film hydration method and two surfactants, span 60 and Tween 80, with more appropriate size, particle size distribution, and encapsulation efficiency which are more suitable in order to reduce the adverse effects of unencapsulated iron.

## Materials and methods

### Materials

The following materials were used in this study: ferrous sulfate heptahydrate (pharmaceutical or food grade), Tween 80 ( $C_{64}H_{124}O_{26}$ ), Span 60 ( $C_{24}H_{46}O_6$ ), cholesterol ( $C_{27}H_{46}O$ ), dichloromethane ( $CH_2Cl_2$ ), and deionized water ( $H_2O$ ). Phosphate buffers, at pH = 6.8 and pH = 5.5, were prepared. All chemicals were purchased from commercial sources, specifically: Merck for Span 60, dichloromethane and ferrous sulfate heptahydrate, PanReac for Tween 80, Sigma for cholesterol, and Semnan Azma for deionized water. The deionized water had a pH in the range of 6.5–7.2 prior to buffer preparation.

### Preparation of niosomes

Niosomes loaded with iron sulfate were prepared by thin film hydration method. Lipid phase components including surfactant and stabilizer were poured into the flask along with 10 cc of dichloromethane solvent and allowed to evaporate the solvent for 1 h by rotary evaporator (HAHNSHIN SCIENTIFIC CO, HAHNVAPOR, HS-2005 V-N, South Korea) at 40 °C and at a speed of 90 rpm (Fig. 1)<sup>28–30</sup>. It was placed under vacuum for 90 min until the residual solvent was completely removed and a solid or lipid layer was observed at the bottom of the flask. Then, during four stages, every ten minutes, 15 cc of the hydration solution including phosphate buffer solution (pH:5.5 or 6.8) along with Iron sulfate (heptahydrate) was added to the flask and after adding the hydration solution in the last step, 20 min was given after which it was sonicated (manufactured by the Ultrasonic Technology Development Company, power 400 watts, frequency 20 kHz) to form the layers of vesicles<sup>31–35</sup>. Moreover, in other process, the phosphate buffer solution and iron sulfate were added in one step to the solid layer formed at the bottom of the flask and the solution was sonicated.

The composition of all formulas, including the ratio of surfactant to stabilizer, the ratio of the mixture of surfactants, the amount of solvent and iron sulfate used in each formula, and the length of time niosomal solution subjected to sonicate are reported in Table 1.

### Physicochemical properties

Once the niosomal solution was prepared, the physical characteristics of the vesicles, such as size and average particle size, drug entrapment efficiency, vesicle sphericity, and zeta potential, which are the main parameters for choosing the most suitable formula, were determined and measured. Thereafter, the results were analyzed by the methods and devices described below.

### Entrapment efficiency

The percentage of iron capture efficiency was determined using atomic absorption. To separate the free iron from the loaded iron, the niosomal solution was centrifuged (FARZANEH ARMAN Co, Iran Bench top high, speed



**Fig. 1.** Vacuum rotary evaporator.

Test number	Chol <sup>a</sup> /1-D <sup>b</sup> : surfactant	Tween80:Span60	Solvent (DCM <sup>c</sup> )	FeSO <sub>4</sub> (7H <sub>2</sub> O)	Ultrasound intensity
F1	(Chol) 1:10	0.75:0.25	10 cc	17 mg	5 min
F2	(Chol) 1:10	1.00:0.00	10 cc	17 mg	5 min
F3	(Chol) 1:10	0.25:0.75	10 cc	17 mg	5 min
F4	(1-D) 0.0266	0.50:0.50	10 cc	17 mg	5 min
F5	(Chol) 1:10	0.50:0.50	10 cc	17 mg	6 min
F6	(Chol) 1:10	0.50:0.50	10 cc	3.5 mg	6 min

**Table 1.** Formulation of iron sulfate-loaded niosomes. a: Cholesterol. b: 1-Dodecanol. c: Dichloromethane.

Test number	Particle size (nm)	PDI <sup>a</sup>	Zeta potential (mV)	EE% <sup>b</sup>
F1	546.8 ± 7.4	0.570 ± 0.05	5.50 ± 0.2	90.80 ± 2
F2	3276 ± 12.3	0.230 ± 0.04	5.06 ± 0.4	93.72 ± 1.5
F3	453.1 ± 7.8	0.590 ± 0.05	6.30 ± 0.7	75.00 ± 1.1
F4	650.9 ± 11.8	0.004 ± 0.001	4.60 ± 0.5	85.30 ± 0.5
F5	558.5 ± 4.9	0.199 ± 0.02	4.01 ± 0.1	82.80 ± 1.7
F6	583.1 ± 5.4	0.365 ± 0.07	-9.91 ± 0.1	83.30 ± 1.4

**Table 2.** Particle size, zeta potential, entrapment efficiency percentage, and PDI of prepared niosomes. a: Polydispersity index. b: Entrapment efficiency.

centrifuge HS 18500R, FAR TEST) for 45 min at 4 °C and at a speed of 10,000 rpm. Next, atomic absorption was taken to determine the efficiency of iron capture. A calibration curve was used to determine the concentration of iron<sup>35</sup>.

In order to ensure that the niosomes were completely precipitated after centrifugation and no vesicles remained in the upper solution and the absorbance would show only the amount of unloaded iron, empty niosomes without iron sulfate were made according to the method mentioned above and centrifuged at different speeds for different periods of time, with UV (SHIMADZU UV-1650 PC, Kyoto, Japan) test performed on the supernatant solution. The supernatant solution, which was centrifuged for 45 min at a speed of 10,000 rpm, showed an absorption number close to zero (0.002), signifying the precipitation of a very large part of niosomes. Accordingly, the best time and speed were selected for centrifugation<sup>36–38</sup>.

The percentage of loaded iron was obtained from Eq. 1:

$$\% EE = \left[ \frac{Fe(t) - Fe(f)}{Fe(t)} \right] * 100 \quad (1)$$

Fe (t): total amount of iron.

Fe (f): amount of free iron.

### Particle size and zeta potential

The diameter of the manufactured niosomes and the dispersion index of these particles can be measured via dynamic light scattering (Malvern, Zetasizer, Nano series, ZS90 with a serial number of MAL1236033, United Kingdom) device. First, 1 cc of the sample for analysis was poured into a suitable container and placed in the machine. After five repetitions, the results of particle size, dispersion index, and zeta potential were determined<sup>39–42</sup>.

### Scanning electron microscopy (SEM)

The structure of the formed niosomes can be identified by a scanning electron microscope (3TESCAN VEGA, Czech Republic). A drop of the sample was poured on a gold-coated aluminum plate and placed under vacuum for 10 min to evaporate the solvent. Then, a photograph of the dried sample was taken and the spherical structure of niosomes was observed<sup>36,37,43</sup>.

### Results and discussion

The results of the measurement of niosomes particles, zeta potential, PDI, and ferrous encapsulation efficiency are presented in Table 2.

The results of this research revealed that adding the hydration solution and hydrating the solid layer step by step or all at once did not affect the characteristics of the vesicles and the efficiency; so, adding the hydration solution in one step shortened the construction time of niosome.

The use of cholesterol and Tween 80 led to the stability and strength of the vesicle wall, which prevents drug leakage. Use of cholesterol in a higher ratio than surfactant causes drug leakage from the vesicle wall<sup>30–34</sup>.

Particle size distribution and particle surface zeta potential were also analyzed for niosome particles loaded with iron sulfate. The average diameter and zeta potential for nano-niosomes lied within the range of 453.1 to 3276 nm and  $-9.91$  to  $6.3$  mV, respectively. Formula F2 had a larger particle size because only Tween 80 surfactant was used, and the addition of Span 60 in other formulas reduced the size of niosomal particles. The size of niosomes depends on the length of the alkyl chain and the hydrophobicity or hydrophilicity of the surfactant. Surfactants with longer alkyl chains create larger vesicles, and hydrophobic surfactants create smaller vesicles. For this reason, Tween 80 alone created large-sized niosomes, and the addition of Span 60, which is the surfactant is hydrophobic, it has reduced the size of the particles.

As mentioned in previous studies, one of the factors influencing the zeta potential is the pH and the concentration of the buffer as a hydration solution<sup>41</sup>. In this study pH 6.8 is the optimal pH for phosphate buffer solution. In PBS buffer, all formulations are surrounded by dense layers of counter-ions which have charges opposite to those of niosomes. The negatively charged ions in PBS buffer bind to partially positive charged hydrogen in cholesterol molecules. The negative charge also comes from hydroxyl groups present in the cholesterol molecules and from an uneven distribution of polarity in non-ionic span 60 – tween 80 surfactants.

In addition, it was observed in this research that one of the other factors affecting the zeta potential is the amount of iron sulfate. In formula F6, due to the lower amount of iron sulfate compared to other formulas, the zeta potential has become a negative number, unlike other results<sup>39–41</sup>.

The entrapment efficiency (EE) and particle size depend on the solubility of the loaded material, the molecular weight of each component of the formulation, and the ratio of each element used in the formulation. The trapping efficiency was within the range of 75–93.72%, with the highest trapping efficiency being related to formula F2, which had the largest particle size. The larger the particle size, the higher the efficiency<sup>40,43</sup>.

PDI is an index to measure the size heterogeneity of molecules or particles in a compound (between 0 and 1). The smaller the PDI, the more homogenous the particle size and the less tendency to agglomerate<sup>41</sup>. F4 Formula, which used 1-Dodecanol as a stabilizer, had the lowest PDI value (0.004) while F3 formula had the highest PDI value (0.59).

Niosome formulations were prepared with phosphate buffer hydration solution with two different pH, where the results of different formulations revealed that the use of phosphate buffer with pH:5.5 in all formulas caused the color to change to orange and ferrous oxidation. However, the use of phosphate buffer with pH:6.8 enhanced efficiency and prevented decomposition as well as color change caused by ferrous oxidation. Figure 2 depicts the comparison of the color of niosome solution due to the use of two different pHs of phosphate buffer<sup>30,44</sup>.

## SEM

After preparing multi-layered niosomes by the dry film hydration method, SEM analysis was performed to ensure the formation of iron-carrying niosomes structure.

According to the SEM images, which are related to the structure and taken from the F1 formulation, it is clear that the niosomes are formed and the desired spherical structures are formed with no agglomeration. SEM images are presented in Fig. 3.

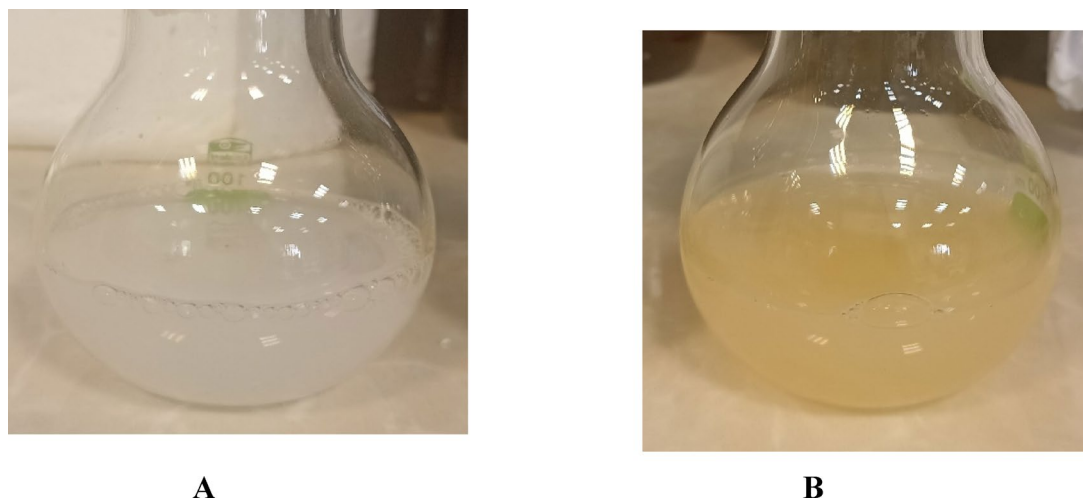


**Fig. 2.** Color comparison of niosomic solution due to the use of two different pHs of phosphate buffer. (A): Niosomes loaded with ferrous with hydration solution pH value 6.8. (B): Niosomes loaded with ferrous with hydration solution pH value 5.5.

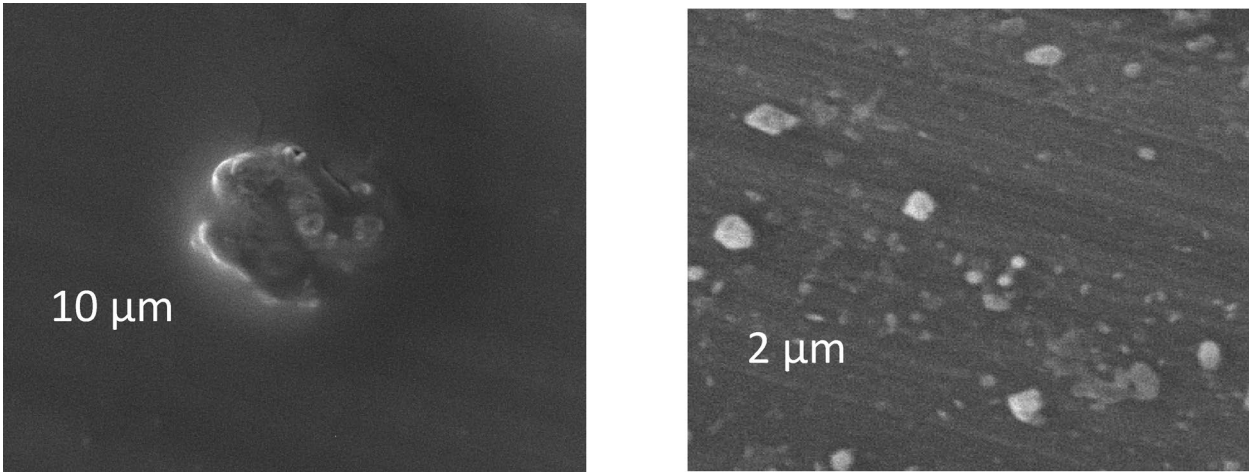


**Fig. 3.** SEM image of niosomes composed of F1 [Tween80:Span60 (0.75:0.25)].

Niosomal system		Z-Average size (nm)		PDI		Zeta potential (mV)		EE (%)	
Previous study	In this study	Previous study	In this study	Previous study	In this study	Previous study	In this study	Previous study	In this study
P <sup>a</sup> -D <sup>b</sup> -Fe <sup>c</sup>	F6	359 ± 5	583 ± 2	0.37 ± 0.03	0.36 ± 0.01	-3 ± 1	-9.9 ± 0.1	75 ± 2	83.3
PO <sup>d</sup> -D-Fe	F4	487 ± 5	650 ± 1	0.41 ± 0.02	0.004 ± 0.001	-52 ± 1	4.6 ± 0.5	72 ± 1	85 ± 1
S80 <sup>e</sup> -D-Fe	F1	826 ± 8	546 ± 1	0.95 ± 0.07	0.57 ± 0.05	-79 ± 2	5.5 ± 0.2	± 284	90 ± 2

**Table 3.** Comparison of the results obtained from this study and the previous study. a: Peceol. b: 1-Dodecanol. c: FeSO<sub>4</sub> (7 H<sub>2</sub>O). d: Plurol Oleique. e: Span 80.

As mentioned earlier, G. Gutiérrez et al. have conducted a study on the loading of iron sulfate in niosomal nanocarriers; in Table 3, we have compared the results obtained from G. Gutiérrez et al.’s research and the findings gained from our research.

According to the results obtained from this study and comparing it with the findings of the previous study conducted by G. Gutiérrez et al., we observe that the size, particle size distribution (PDI), and entrapment efficiency of F1 formula have been improved compared to the S80-D-Fe formula. The entrapment efficiency rose from 84 to 90%, the particle size diminished from 826 nm to 546 nm, and the PDI dropped from 0.95 to 0.57, meaning that PDI indicates the particle size homogeneity.

In formula F4, PDI and efficiency have been improved compared to the results obtained from the previous study. In formula F6, compared to the previous study, the zeta potential and efficiency have been improved.

In addition to improving the entrapment efficiency, particle size distribution and vesicle size, in this research, we were able to shorten the stages and time of niosome preparation without hurting the physical and chemical parameters of niosomes. Also, by comparing and conducting the experiment, we should provide the appropriate pH for the phosphate buffer hydration solution to prevent from iron oxidation<sup>45–50</sup>.

Conclusion

Consuming iron freely causes problems such as oxidation, poor bioavailability, poor intestinal absorption, etc. As such, its encapsulation prevents from occurrence of such problems. So far, iron encapsulation in a liposomal nanocarrier has been able to overcome these problems to some extent, but this nanocarrier is not sufficient for the reasons mentioned before, and we presented a more efficient method with lower cost, flexible formulation, and easy fabrication.

In this study, it was shown for the first time that the niosomal formula including surfactant Tween 80 and Span 60 (0.75:0.25), the 1:10 cholesterol to surfactant ratio, and 1 mM as the amount of ferrous sulfate can be a suitable formula for loading iron. Also, by shortening the steps and the hydration time without negative effect on the physical and chemical properties of the niosomal nanocarrier, finally iron sulfate was loaded in the niosomal nanocarrier with 90.8% trapping efficiency with a particle size of 546.8 nm.

In general, the results of this research suggest that if the problem of niosomes’ instability and accumulation is solved by methods such as the addition of charge induction or appropriate formulation, they can be a suitable nanocarrier for loading various drugs, supplements, including iron sulfate for the treatment of anemia and lack of iron. They can also be a suitable alternative for other nanocarriers such as liposomes without problems such as toxicity, high cost, etc., and with its commercialization, they can help treat many diseases, including anemia.



## Data availability

Data is provided within the manuscript (Include original data generated in my research).

Received: 27 January 2025; Accepted: 26 May 2025

Published online: 06 June 2025

## References

- Wang, J., & Pantopoulos, K. regulation of cellular iron metabolism. *Biochem. J.*, **434**(3), 365–381.
- Denic, S. & Agarwal, M. M. Nutritional iron deficiency: an evolutionary perspective. *Nutrition* **23**, 603–614. <https://doi.org/10.1016/j.nut.2007.05.002> (2007).
- Cancelo-Hidalgo, M. J. et al. Tolerability of different oral iron supplements: a systematic review. *Curr. Med. Res. Opin.* **29**, 291–303. <https://doi.org/10.1185/03007995.2012.761599> (2012).
- Caetano-Silva, M. E. et al. synthesis of Whey peptide-iron complexes: influence of using different iron precursor compounds. *Food Res. Int.*, **101**, 73–81. <https://doi.org/10.1016/j.foodres.2017.08.056>
- Gandhi, K. et al. Enhanced bioavailability of iron from spray dried Whey protein concentrate-iron (WPC-Fe) complex in anaemic and weaning conditions. *J. Funct. Foods*, **58**, 275–281. <https://doi.org/10.1016/j.jff.2019.05.008> (2019).
- Onsekizoglu Bagci, P. & Gunasekaran, S. Iron-encapsulated cold-set Whey protein isolate gel powder – Part 1: optimisation of Preparation conditions and in vitro evaluation. *Int. J. Dairy Technol.* **70** (1), 127–136. <https://doi.org/10.1111/1471-0307.12317> (2017).
- Berdanier, C. D., Berdanier, L. A. & Zempleni, J. Advanced Nutrition: Macronutrients, Micronutrients, and Metabolism. CRC.
- Gutiérrez, G. et al. Iron-entrapped niosomes and their potential application for yogurt fortification. *LWT* **74**, 550–556 (2016).
- Gahrue, H. H., Eskandari, M. H., Mesbahi, G. & Hanifpour, M. A. Scientific and technical aspects of yogurt fortification: A review. *Food Sci. Hum. Wellness*, **4**, 1–8. <https://doi.org/10.1016/j.fshw.2015.03.002> (2015).
- Camaschella, C. Iron deficiency. *Blood. J. Am. Soc. Hematol.* **133** (1), 30–39 (2019).
- Elstrott, B., Khan, L., Olson, S., Raghunathan, V., DeLoughery, T., & Shatzel, J. The role of iron repletion in adult iron deficiency anemia and other diseases. *European J. Haematol.*, **104** (3), 153–161. (2020).
- Prichapan, N., McClements, D. J. & Klinkesorn, U. Iron encapsulation in water-in-oil emulsions: effect of ferrous sulfate concentration and fat crystal formation on oxidative stability. *J. Food Sci.* **83** (2), 309–317 (2018).
- Wardhani, D. H., Aryanti, N., Aziz, A., Firdhaus, R. A. & Ulya, H. N. ultrasonic degradation of alginate: A matrix for iron encapsulation using gelation. *Food Biosci.* **41**, 100803 (2021).
- Zimmermann, M. B. The potential of encapsulated iron compounds in food fortification: a review. *Int. J. Vitam. Nutr. Res.* **74**, 453–461 (2004).
- Katuwawila, N. P. et al. Alginate nanoparticles protect ferrous from oxidation: potential iron delivery system. *Int. J. Pharm.* **513** (1–2), 404–409. <https://doi.org/10.1016/j.ijpharm.2016.09.053> (2016).
- Kazemi-Taskooh, Z. & Varidi, M. Designation and characterization of cold-set whey protein-gellan gum hydrogel for iron entrapment. *Food Hydrocolloids*, **111**, Article 106205. (2020). <https://doi.org/10.1016/j.foodhyd.2020.106205>. May 2020.
- Ulya, H. N., Wardhani, D. H., Aryanti, N. & Pangestuti, D. R. Deacetylation of glucomannan of *Amorphophallus oncophyllus* using NaOH and its properties as iron excipient by gelation in ethanol. AIP Conference Proceedings. <https://doi.org/10.1063/1.5139864>
- Uchegbu, I. & Vyas, S. P. Non-ionic surfactant based vesicles (niosomes) in drug delivery. *Int. J. Pharm.* **172**, 33–70. [https://doi.org/10.1016/S0378-5173\(98\)00169-0](https://doi.org/10.1016/S0378-5173(98)00169-0) (1998).
- Kopermsub, P., Mayen, V. & Warin, C. Potential use of niosomes for encapsulation of Nisin and EDTA and their antibacterial activity enhancement. *Food Res. Int.* **44**, 605–612. <https://doi.org/10.1016/j.foodres.2010.12.011> (2010).
- Devaraj, G. N. et al. Release studies on niosomes containing fatty alcohols as bilayer stabilizers instead of cholesterol. *J. Colloid Interface Sci.* **251**, 360–365 (2022). <http://www.ncbi.nlm.nih.gov/pubmed/16290741>
- Marianecci, C. et al. Niosomes from 80s to present: the state of the Art. *Adv. Colloid Interface Sci.* **205**, 187–206. <https://doi.org/10.1016/j.cis.2013.11.018> (2013).
- Kazemi-Taskooh, Z. & Varidi, M. Food-based iron delivery systems: A review. *Trends Food Sci. Technol.* **116**, 75–89 (2021).
- Behnam, B. et al. Microniosomes for concurrent doxorubicin and iron oxide nanoparticles loading: preparation, characterization and cytotoxicity studies. *Artificial Cells Nanomed. Biotechnol.* **46** (1), 118–125.
- Khaleghian, M. et al. B. & In Silico design and mechanistic study of niosome-encapsulated Curcumin against multidrug-resistant *Staphylococcus aureus* biofilms. *Front. Microbiol.*, **14**, 1277533.
- Paseban, K. et al. A. Aryan Tavana and T. Piri Gharaghie, Preparation and optimization of niosome encapsulated meropenem for significant antibacterial and anti-biofilm activity against methicillin-resistant 438 *Staphylococcus aureus* isolates. *Heliyon*. **10** (2024).
- Rezaei, H., Iranbakhsh, A., Akhavan Sepahi, A., Mirzaie, A. & Larijani, K. Formulation, Preparation of niosome loaded zinc oxide nanoparticles and biological activities. *Sci. Rep.*, 16692, (2024).
- Abbasi, M. et al. Color change of primary teeth following exposure to an experimentally synthesized liposomal nano encapsulated ferrous sulfate drop versus the commercially available iron drops. *Pediatr. Dent. J.*, **31**(3), 256–267.
- Machado, N. D., Silva, O. F., de Rossi, R. H. & Fernández, M. A. cyclodextrin modified niosomes to encapsulate hydrophilic compounds. *RSC Adv.*, **8**(52), 29909–29916. (2018).
- García-Manrique, P. et al. Effect of drug molecular weight on niosomes size and encapsulation efficiency. *Colloids Surf., B*, **186**, 110711 (2020).
- Cengiz, A., Schroën, K. & Berton-Carabin C. Towards oxidatively stable emulsions containing iron-loaded liposomes: the key role of phospholipid-to-iron ratio. *Foods*, **10** (6), 1293 (2021).
- Ding, B., Xia, S., Hayat, K. & Zhang, X. Preparation and pH stability of ferrous glycinate liposomes. *J. Agric. Food Chem.* **57**, 2938–2944 (2009).
- Cengiz, A. Ferrous Sulfate Nanoencapsulation with Liposome and Emulsification Methods and the Usage in Cocoa Containing Nut Paste. Master's Thesis, Ondokuz Mayıs University, Samsun, Turkey, (2013).
- Keller, B. C. Liposomes in nutrition. *Trends Food Sci. Technol.* **12**, 25–31 (2001).
- Lu, X. Y., Hu, S., Jin, Y. & Qiu, L. Y. Application of liposome encapsulation technique to improve anti-carcinoma effect of Resveratrol. *Drug Dev. Ind. Pharm.* **38**, 314–322 (2012).
- Bochicchio, S., Dalmoro, A., Lambert, G. & Barba, A. advances in nanoliposomes production for ferrous sulfate delivery. *Pharmaceutics*, **12**(5), 445 (2020).
- Mohamad, E. A. & Fahmy, H. M. Niosomes and liposomes as promising carriers for dermal delivery of *Annona squamosa* extract. *Brazilian J. Pharm. Sci.*, **56**, e18096. (2020).
- Morteza-Semnani, K. et al. Preparation and in-vitro evaluation of ketoconazole-loaded niosome (ketosome) for drug delivery to cutaneous candidiasis. *Pharm. Sci.* **29** (2), 208–218 (2022).
- Hashim, F., Elkhateeb, D., Ali, M. M. & Abdel-Rashid, R. S. Effect of formulation variables and bile salts addition on entrapment efficiency of Curcumin loaded niosomes. *J. Adv. Pharm. Res.*, **6** (3), 123–132. (2020).

39. Zhang, Y. et al. Sodium Dodecyl sulfate improved stability and transdermal delivery of solidoside-encapsulated niosomes via effects on zeta potential. *Int. J. Pharm.* **580**, 119183 (2020).
40. Owodeha-Ashaka, K., Ilomuanya, M. O. & Iyire, A. Evaluation of sonication on stability-indicating properties of optimized pilocarpine hydrochloride-loaded niosomes in ocular drug delivery. *Prog. Biomater.* **10**, 207–220 (2021).
41. Guimarães, D., Cavaco-Paulo, A. & Nogueira, E. Design of liposomes as drug delivery system for therapeutic applications. *Int. J. Pharm.* **601**, 120571 (2021).
42. Talebi, V., Ghanbarzadeh, B., Hamishehkar, H., Pezeshki, A. & Ostadrahimi, A. Effects of different stabilizers on colloidal properties and encapsulation efficiency of vitamin D3 loaded nano-niosomes. *J. Drug Deliv. Sci. Technol.* **61**, 101284 (2021).
43. Usman, M. R. M., Ghuge, P. R. & Jain, B. V. Niosomes: a novel trend of drug delivery. *Eur. J. Biomedical Pharm. Sci.*, **4**(7), 436–442 (2017).
44. Xia, S. & Xu, S. Ferrous sulfate liposomes: preparation, stability and application in fluid milk. *Food Res. Int.* **38** (3), 289–296 (2005).
45. Rost, N. C. V. et al. Magnetic particle imaging performance of liposomes encapsulating iron oxide nanoparticles. *J. Magn. Magn. Mater.*, 166675.
46. Elmi, N. et al. Physical properties and stability of Quercetin loaded niosomes: stabilizing effects of phytosterol and polyethylene glycol in orange juice model. *J. Food Eng.* **296**, 110463 (2021).
47. Nada, K. et al. A. Letrozole-loaded nonionic surfactant vesicles prepared via a slurry-based proniosome technology: formulation development and characterization. (2020).
48. Rasul, A. et al. S. in vitro characterization and release studies of combined nonionic surfactant-based vesicles for the prolonged delivery of an immunosuppressant model drug. *Int. J. Nanomed.*, 7937–7949. (2020).
49. Shah, J. et al. Enhancement in antinociceptive and anti-inflammatory effects of Tramadol by transdermal proniosome gel. *Asian J. Pharm. Sci.*, **15**(6), 786–796. (2020).
50. Sadeghi, S. et al. Design and physicochemical characterization of lysozyme loaded Niosomal formulations as a new controlled delivery system. *Pharm. Chem. J.*, **53**, 921–930. (2020).

## Acknowledgements

We would like to acknowledge the Semnan University of Iran for their supports.

## Author contributions

Authorship contribution statement Samira Khalilabadi: Data curation, Conceptualization, Investigation, Methodology, Validation, Writing – original draft. Kiana Peyvandi: Writing – review & editing, Supervision, Project administration, Funding acquisition. Sheida Shariat: Writing – review & editing, Supervision.

## Declarations

## Competing interests

The authors declare no competing interests.

## Additional information

**Correspondence** and requests for materials should be addressed to K.P.

**Reprints and permissions information** is available at [www.nature.com/reprints](http://www.nature.com/reprints).

**Publisher's note** Springer Nature remains neutral with regard to jurisdictional claims in published maps and institutional affiliations.

**Open Access** This article is licensed under a Creative Commons Attribution-NonCommercial-NoDerivatives 4.0 International License, which permits any non-commercial use, sharing, distribution and reproduction in any medium or format, as long as you give appropriate credit to the original author(s) and the source, provide a link to the Creative Commons licence, and indicate if you modified the licensed material. You do not have permission under this licence to share adapted material derived from this article or parts of it. The images or other third party material in this article are included in the article's Creative Commons licence, unless indicated otherwise in a credit line to the material. If material is not included in the article's Creative Commons licence and your intended use is not permitted by statutory regulation or exceeds the permitted use, you will need to obtain permission directly from the copyright holder. To view a copy of this licence, visit <http://creativecommons.org/licenses/by-nc-nd/4.0/>.

© The Author(s) 2025